ISSN: 2277-3754
ISO 9001:2008 Certified
International Journal of Engineering and Innovative Technology (IJEIT)
Volume 3, Issue 1, July 2013

Effect of Lateral Jet Interaction with External Flow at Positive and Negative Incidence

S.Srinivas Prasad, K.Durga Rao, R.K.Sharma, G.V.Ramana Murty

Abstract*— Numerical study is performed on spherically blunted cone with a circular air jet injected at right angles to the body surface from leeward side. Three dimensional Navier-Stokes equations along with k-ω SST turbulence model are solved using commercial CFD software. Computed surface pressure has been compared with the test data available in open literature published by Kurita (2000) with jet-off and jet-on conditions at zero degree angle of attack, with 8.1 Mach number. The results are in good agreement with the experimental data. Numerical study has been carried out to examine the flow fields, pressure distribution and the effect of jet interaction on the resulting aerodynamics of reentry vehicle at $\alpha = 10^0$ and -10^0. Normal force coefficient value decreased by 14.2% when compared with jet-off condition at $\alpha = 10^0$ and increased by 30% with $\alpha = -10^0$. Pitching moment coefficient is decreased by 17.08% at $\alpha = 10^0$ and increased by 35.8% with $\alpha = -10^0$. Even though the jet interaction is strong at $\alpha = -10^0$, the interaction force and moment produced by jet interaction acts opposite to the jet thrust. But the jet interaction force and moment augment the jet thrust at $\alpha = 10^0$. Therefore, the leeward jet with positive angle of attack enhances jet force and moment. The magnitude, direction of the forces and moments acting with jet-off and jet-on conditions have been quantified for different flight and jet conditions.

***Index Terms*— Aerodynamics, CFD, Hypersonic Flow, Reentry vehicle.**

NOMENCLATURE

A = Angle of attack
M_∞ = Mach number
C_N = Normal force coefficient
X_{cp} = Centre of Pressure
C_A = Axial force coefficient
C_m = Moment coefficient
JPR = Jet pressure ratio
p = Static Pressure
T = Temperature
p_∞ = Free stream Pressure
d = Reference diameter
X_{cp}/d = C_m/C_N

I. INTRODUCTION

The lateral jets are also called as reaction control systems are employed to control the re-entry vehicle. The lateral jet control has quick control for a re-entry vehicle and is effective to make corrections for the disturbances encountered during ascent and descent phase in the trajectory. Reentry vehicles often do not have aerodynamic control surfaces. Even reentry vehicle employed aerodynamic surfaces for control during reentry, will be ineffective because of very low dynamic pressure at higher altitude. Therefore, the reaction control system is still important to control the vehicle. At higher altitudes, lateral jets offer the only possibility to exert sufficient control forces for reentry vehicle. When lateral jets are operated within atmosphere, the net force applied on the vehicle may be influenced by interactions between the jet and the external stream. The interaction of a lateral jet with the external flow creates a significant surface pressure field. The lateral force generated by this pressure field augments the jet thrust and thus increases the effectiveness of the jet. An accurate prediction of the resulting aerodynamic force is difficult because the flow field around such a jet in cross flow is rather complex. In addition to the jet thrust a considerable pressure load on the body can be generated by the jet/cross flow interactions. Flight and jet conditions and configuration parameters have an effect on the flow interaction pressure force. However, the main objective of the present study is to understand the effect of jet interaction at $\alpha = 10^0$ and -10^0.

II. BODY GEOMETRY CONSIDERED IN THE PRESENT INVESTIGATION

The reentry configuration used in the present study is a spherically blunted cone having 10.3^0 semi apex angle with a bluntness ratio of 0.523. The lateral jet is turned off and the jet is considered as a wall. This condition is called jet-off condition in the present study. The body geometry used and the direction of normal and axial forces are shown in Fig 1. The diameter of the lateral jet is 2 mm and is at a distance of 0.33d from base on leeward side.

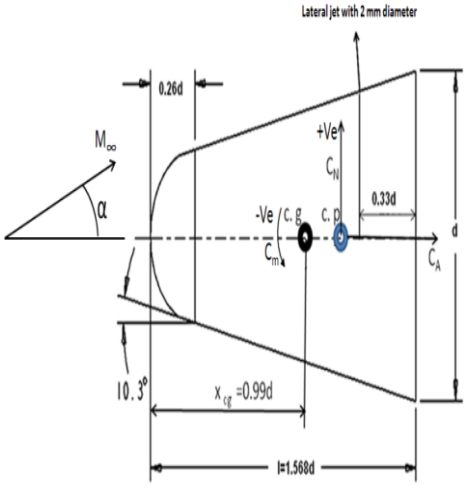

Fig 1 Schematic View of Model with Sign Convection Used For Normal Force and Pitching Moment

ISSN: 2277-3754
ISO 9001:2008 Certified
International Journal of Engineering and Innovative Technology (IJEIT)
Volume 3, Issue 1, July 2013

III. GRID GENERATION

The geometry and structured mesh were created using the grid generation software Gambit 2.4.6 supplied in FLUENT software suite. A parabolic computational domain is created around the reentry body. Computational domain has been considered such that the outer boundary does not interfere with the jet flow. The physical domain under consideration is shown in Fig 2 which consists of the reentry body and fluid domain. Hexahedral cells are used in the entire domain. Grid points were concentrated more near the jet exit in order to resolve the larger gradient in flow variables. In generating the mesh, boundary layer mesh spacing was used near the reentry body surface. Fine mesh is used near the jet and growth rate has been maintained away from the body.

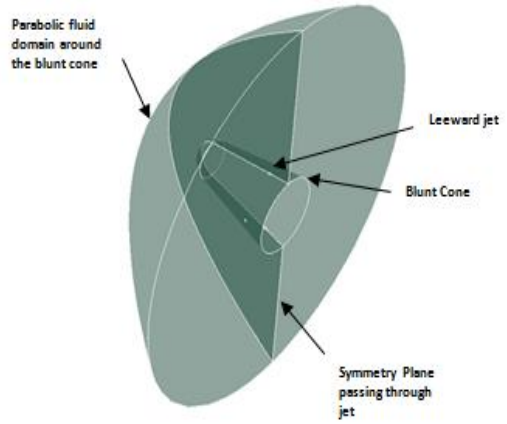

Fig 2 Fluid Domain around Vehicle

IV. GOVERNING EQUATIONS OF FLUID FLOW

The CFD code models the conservation equations of mass, momentum and energy in terms of the dependent variables (Velocity, pressure and enthalpy). They are time dependent in a turbulent flow. These quantities are decomposed into a mean component and a fluctuating one and the original conservation equations are converted to an averaged form. For compressible flows, the mean form of equations is obtained through a time-averaging process, usually called Reynolds stress averaging and a technique of mass averaging, also called Favre averaging. The original equations for the conservations of mass, momentum and energy are expressed in terms of time and Favre averaged quantities. The momentum and energy equations contain terms that cannot be expressed as function of the mean flow variables which are the Reynolds stresses, the turbulent energy fluxes and the fluctuating viscous work term. These terms are related to known quantities by using a turbulence model before a close solution of the equations becomes possible. The governing equations of a compressible turbulent flow can be written using time-averaged (Reynolds-averaged, indicated by an overbar) values of the density, pressure and mass- weighted (Favre-averaged, indicated by a tilde) averages for the Velocity components and Temperature. Prime indicates the fluctuating component coming from the mass-averaged process. Double prime indicates the fluctuating component coming from the mass averaged process.

The governing equations used in this study are presented in their differential form.

Conservation of mass,

$$\frac{\partial \bar{\rho}}{\partial t} + \frac{\partial (\bar{\rho}\tilde{u}_j)}{\partial x_j} = 0 \qquad \text{Eq. 1}$$

Conservation of momentum

$$\frac{\partial \bar{\rho}\tilde{u}_i}{\partial t} + \frac{\partial (\bar{\rho}\tilde{u}_j\tilde{u}_i)}{\partial x_j} = -\frac{\partial \bar{p}}{\partial x_i} + \frac{\partial}{\partial x_j}\left[\mu\left(\frac{\partial \tilde{u}_i}{\partial x_j} + \frac{\partial u_j}{\partial x_i} - \frac{2}{3}\delta_{ij}\frac{\partial \tilde{u}_l}{\partial x_l}\right)\right] + \frac{\partial}{\partial x_j}\left(-\bar{\rho}\,\widetilde{u''_i u''_j}\right) \qquad \text{Eq. 2}$$

The above equation contains term that cannot be expressed as a function of the mean flow variables. This term is called Reynolds stress tensor defined by $(-\bar{\rho}\,\widetilde{u''_i u''_j})$. Boussinesq hypothesis is used to relate the Reynolds stresses to the mean velocity gradients. The advantage of this approach is the relatively low computational cost associated with the computation of the turbulent viscosity (μ_t).

$$-\bar{\rho}\,\widetilde{u''_i u''_j} = \mu_t\left(\frac{\partial \tilde{u}_i}{\partial x_j} + \frac{\partial u_j}{\partial x_i}\right) - \frac{2}{3}\delta_{ij}\left(\rho k + \mu_t \frac{\partial u_k}{\partial x_k}\right) \qquad \text{Eq. 3}$$

Conservation of energy,

$$\frac{\partial \bar{\rho} e_0}{\partial t} + \frac{\partial (\bar{\rho} e_0 \tilde{u}_j + \bar{p}\tilde{u}_j + \bar{\rho}\widetilde{e''_0 u''_j})}{\partial x_j} = \frac{\partial [(-\bar{p}\,\widetilde{u''_i u''_j})\tilde{u}_i]}{\partial x_j} - \frac{\partial (\overline{q_i})}{\partial x_j} \qquad \text{Eq. 4}$$

Where $e_0 = \overline{C_v T} + \frac{1}{2}\tilde{u}_j\tilde{u}_j + \frac{1}{2}\widetilde{u''_j u''_j}$ Eq. 5

SST k-ω Turbulence Model

The shear stress transport k-ω model is the only variation of the standard k-ω model available in FLUENT. It was developed by Menter (1994) using the standard k-ω model and a transformed k-epsilon model. The main difference is the way in which the model calculates the turbulent viscosity to account for the transport of the principal turbulent shear stress. This model also incorporates a cross-diffusion term in the ω equation and a blending function to allow proper calculation of the near-wall and far-field areas. The blending function triggers the standard k-ω model in near wall regions and triggers the k-ε like model in areas away from the surface. These differences make the SST model more precise for a larger variety of flows than the standard model.

Similar to the standard k-ω model, the transport equations for k and ω are slightly modified and are given by

$$\frac{\partial (\rho k)}{\partial t} + \frac{\partial (\rho k u_i)}{\partial x_i} = \frac{\partial}{\partial x_j}\left[\left(\mu + \frac{\mu_t}{\sigma_k}\right)\frac{\partial k}{\partial x_j}\right] + \widetilde{G_k} - Y_k + S_k \qquad \text{Eq. 6}$$

$$\frac{\partial (\rho \omega)}{\partial t} + \frac{\partial (\rho \omega u_i)}{\partial x_i} = \frac{\partial}{\partial x_j}\left[\left(\mu + \frac{\mu_t}{\sigma_\omega}\right)\frac{\partial k}{\partial x_j}\right] + G_\omega - Y_\omega + D_\omega + S_\omega \qquad \text{Eq. 7}$$

Where $\widetilde{G_k}$ represents the generation of turbulent kinetic energy arises due to mean velocity gradients, G_ω is generation of ω and Y_k and Y_ω represent the dissipation of k and ω due to turbulence. α_k and α_ω are the turbulent Prandt1 numbers for k and ω respectively and S_ε and S_k are source terms defined by the user. D_ω is the cross-diffusion term.

V. FLOW SOLVER DESCRIPTION

Commercial CFD software FLUENT is used for the simulation. The simulation has been performed with an

ISSN: 2277-3754
ISO 9001:2008 Certified
International Journal of Engineering and Innovative Technology (IJEIT)
Volume 3, Issue 1, July 2013

implicit compressible flow solver. The flow field is assumed to be compressible and turbulent. CFD studies are carried out to determine the flow and aerodynamic coefficients on the selected reentry configuration. The implicit, compressible (coupled) solver was used. The shear stress transport k-omega two equation model was used for the flow variables and the turbulent viscosity equation. The initial conditions were set to the previously defined free stream conditions and are applicable to all simulations in this study.

VI. BOUNDARY CONDITIONS

A far-field boundary condition is used in FLUENT to model a free stream condition at inlet to domain with free stream Mach number at $\alpha = 5^0$ and static conditions. The Mach number (M_∞ = 6, 8.1, 12, 16), the static temperature ($T\infty = 267.3$ K) and the static pressure ($P\infty = 550$ Pa) are used for external flow simulation. Turbulent viscosity is defined as 1% of the free stream at inlet. Mass flow boundary condition is used to provide a prescribed jet mass flow rate or mass flux distribution at a jet inlet. Mass flow rate at the jet exit is 0.068 kg/s and the jet pressure is 0.64 MPa. Pressure outlet boundary condition is used to define the static pressure at domain outlet. The re-entry vehicle body wall was modeled as no-slip condition. Iterative procedure requires that all solution variables be initialized before calculating a solution. Initialize the entire flow field using the values set for far-field in the present study. A symmetry boundary condition applies to the symmetry plane of the problem.

VII. JET INTERACTION WITH POSITIVE AND NEGATIVE INCIDENCE ($\alpha = 10^0$ AND -10^0)

Numerical study has been carried out to examine the flow fields at incidences ($\alpha = 10^0$ and -10^0) and the effect of jet interaction on the resulting aerodynamics of the flight vehicle. Mach contours are compared in Fig 4. There is a drastic change in the flow pattern both on the surface and in pitch plane. The jet is penetrating more into free stream and part of the jet stream can move upstream into the recirculation region at 10^0 incidence while the jet stream is bending toward downstream at $\alpha = -10^0$.

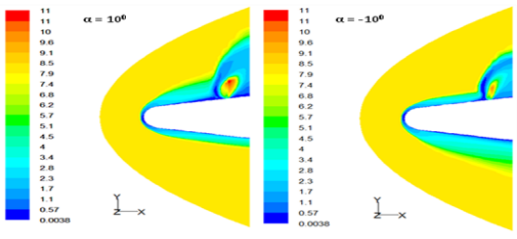

Fig 4 Mach Contours At A =10^0 and A =

The jet displaces the shock farther from the body at positive incidence and is pushed inward to the body at negative incidence. The recirculation region upstream of jet is larger at positive incidence and smaller at negative incidence. At $\alpha = -10^0$ there is a strong interference between the detached bow shock and jet. This interference between the detached bow shock and the jet with variation in angle of attack is important and quantified. The induced jet interaction surface pressure has been compared in Fig .5 It indicates that the peak pressure at x/d = 1.16 with $\alpha = -10^0$ is higher than peak pressure with $\alpha = 10^{0.}$

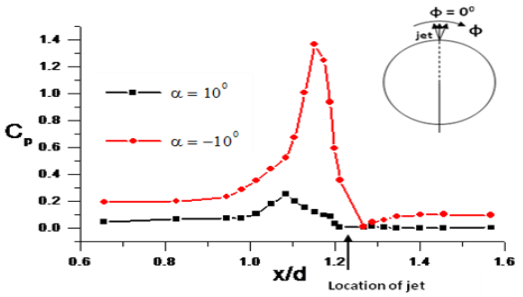

Fig 5 Longitudinal Pressure Distribution In Jet Interaction Area X/D = (0.6 To 1.568)

The circumferential pressure distribution is plotted in Fig 6. In case of $\alpha = 10^0$ the interference effects between the main bow shock and jet are minimal where as in case of $\alpha = -10^0$, the pressures experienced close to the jet are high when compared to $\alpha = 10^0$. This indicates that at $\alpha = -10^0$, the jet interaction force augments the jet thrust.

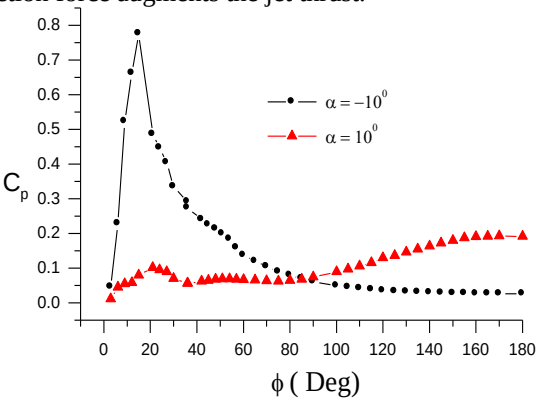

Fig 6 Circumferential Pressure Distribution In A Plane Passing Through Centre Of Jet At (X/D = 1.236) , $M_\infty = 8.1$, A = 5^0, JPR = 1100, Jet Mass Flow

For jet-off condition, the lateral jet is turned off in present study and the jet is considered as a wall. Only external flow over the vehicle has been considered for jet-off condition and lateral jet operating conditions and their interaction effects have been not considered. The normal force coefficient distribution obtained with $\alpha = 10^0$ and $\alpha = -10^0$ are compared in Fig 7 to understand the effectiveness of jet. The normal force coefficient with $\alpha = 10^0$ is positive and $\alpha = -10^0$ is negative. C_N distribution till x/d = 0.9 is almost same for both cases. The distribution is changed between x/d = 0.9 to 1.56. Due to jet interaction C_N value is decreased by 14.2% when compared with jet-off condition at $\alpha = 10^0$ and increased by 30% with $\alpha = -10^0$. C_m value is decreased by 17.08% at $\alpha = 10^0$ and C_m value is increased by 35.8% with $\alpha = -10^0$. Even though the jet interaction is strong at $\alpha = -10^0$, the interaction

ISSN: 2277-3754
ISO 9001:2008 Certified
International Journal of Engineering and Innovative Technology (IJEIT)
Volume 3, Issue 1, July 2013

force and moment produced by jet interaction acts opposite to the jet thrust. But the jet interaction force and moment augment the jet thrust at $\alpha = 10^0$. Therefore, the leeward jet with positive angle of attack enhances jet force and moment. The resulting aerodynamic coefficients have been compared in Table 1.

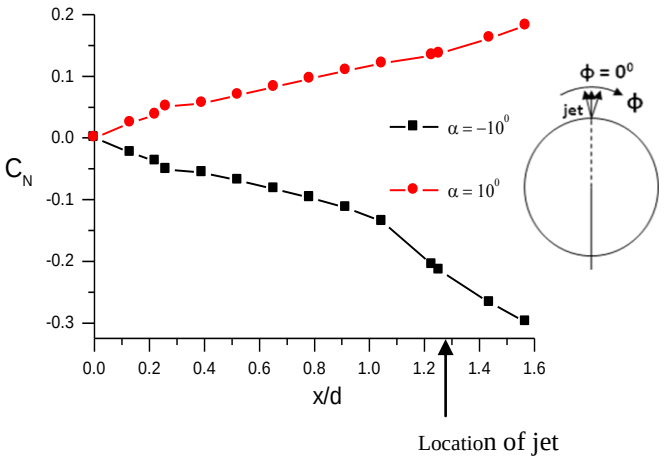

Fig-7 Longitudinal Normal Force Coefficient Distribution On Leeward Surface ($\Phi = 0^0$) With Jet-On Condition At $M_\infty = 8.1$, JPR= 1100, Altitude = 35 Km

Table 1 Comparison of C_N and C_m at $M\infty = 8.1$, A = 10^0 and A = -10^0

α	Jet Location	C_N	C_m	X_{cp}/d
10	Jet off	0.21	-0.193	0.92
-10	Jet off	-0.21	0.1925	0.9
10	Jet on	0.18	-0.16	0.86
-10	Jet on	-0.3	0.3	1

VIII. CONCLUSION

This study helps to understand the lateral jet interaction with eternal flow at $\alpha = 10^0$ and $\alpha = -10^0$. The upstream length of the interaction region increases with the angle of attack but its lateral spreading decreases with the angle of attack. It can be seen that the jet force augmented by the jet interaction force acting ahead of the jet. The jet interaction force augment the jet thrust at $\alpha = 10^0$

REFERENCES

[1] Champigny, P, and Lacau. R. G, "Lateral jet Control for tactical Missiles," Special course on missile aerodynamics, AGARD-FDP Von Karman Institute, Brussels, Belgium, 6-10 June 1994, pp. 3.1-3.57.

[2] Srivastava.B .B "Computational analysis and validation for lateral jet controlled Missiles "Journal of space craft and rockets" Vol.34, No.5, September-October 1997.

[3] Hsieh. T, Computational and experimental analysis of cross jet interaction flow fields of a bi-conic body at incidences. AIAA-98-2625.

[4] Kurita.M, Tsuyoshi Inoue and Nakamura.Y "Aerodynamic interaction due to side jet from a blunted cone in hypersonic flow"AIAA-2000-4518.

[5] Kurita.M, Okada .T and Nakamura.Y "The Effects of attack angle on aerodynamic interaction due to side jet from a blunted body in a supersonic flow" AIAA 2001-0261.

[6] Kurita.M, Okada .T and Nakamura.Y" The Effects of attack angle on side jet aerodynamic interaction in blunted body at hypersonic flow."AIAA 2001-1825.

[7] Kennedy .K, Walker. B and Michelson's "Jet interaction effects on a missile with aerodynamic control surfaces" AIAA Paper 99-0807, January 1999.

[8] Gimelshein S.F, Alexeenko A.A. and Levin D.A. "Modeling of the interaction of a side jet with a rarefied atmosphere "Journal of spacecraft and rockets "Vol.39, No.2, March-April 2002.

[9] Tetsuya Nakamura, Munetsugu Kaneko, Igor Menshov and Yoshiaki Nakamura" Numerical simulation on aerodynamic interaction between a side jet and flow around a blunt body in hypersonic flow" AIAA - 2003-1135.

[10] Valerio Viti Joseph Schetz and Reece Neel" Comparison of first and second Order turbulence models for a Jet/3D ramp combination in supersonic flow" AIAA 2005-1100.